Microchemical Journal 218 (2025) 115124

Contents lists available at ScienceDirect

Microchemical Journal

journal homepage: www.elsevier.com/locate/microc

Development of a triabody-based immunoassay against a pathogenic epitope in human ApoB100 for the diagnosis and monitoring of atherosclerosis

Juncheng Wang [a,b,c,1], Meng Liu [b,1], Rukhshan Zahid [b], Wenjie Zhang [d], Jiasheng Hao [b], Yuekang Xu [a,b,*]

[a] Xinjiang Key Laboratory of Biological Resources and Genetic Engineering, College of Life Science and Technology, Xinjiang University, Urumqi 830017, China
[b] Anhui Provincial Key Laboratory for Conservation and Exploitation of Biological Resources, College of Life Sciences, Anhui Normal University, Wuhu, Anhui 241000, China
[c] School of Basic Medicine, Nanchang Medical College, Nanchang, Jiangxi 330052, China
[d] The First Affiliated Hospital of Wannan Medical College, Wuhu, Anhui 241001, China

ARTICLE INFO

Keywords:
Atherosclerosis
ApoB 100
p210
Epitope
Immunoassay

ABSTRACT

Cardiovascular diseases are the number one deadly diseases worldwide, with atherosclerosis being their pathological basis. However, the development of atherosclerosis is chronic and asymtomatic, posing significant challenges for its early detection and timely treatment. Recently, a 3136–3155 amino acid sequence, p210, in the apolipoprotein B-100 (ApoB100) of low density lipid was found to be associated with the severity of atherosclerosis and the risk of cardiovascular events. To develop a precise and sensitive immunoassay for the early diagnosis of atherosclerosis, three phage libraries displaying single chain fragment variable (scFv) against the p210 peptide in human ApoB100 were constructed in the present study, and three high affinity scFvs obtained, which were then genetically engineered to constitute a triabody that significantly enhanced its functional affinity and antigen-capturing capability towards the pathogenic p210 peptides. Furthermore, a rapid and simple method was developed with the triabody for early monitoring of the disease progression in clinical settings. The linear range of the sandwich ELISA containing the triabody was 36–576 ng/mL, with a limit of detection of 28.5 ng/mL. In addition, the average recovery of intra- and inter-assay were 88.4 ± 3.0 % and 85.5 ± 5.2 %, respectively. The developed assay was highly sensitive and specific for the pathogenic epitope, and no cross-reactivity with other antigens in serum observed. Importantly, since the triabody developed with trimeric scFvs against the same epitope has 2.5 times higher affinity than that of normal antibody with monomeric scFv, its derived sandwich ELISA could measure the amounts of pathogenic epitopes at very low levels, thereby capable of detecting signals corresponding to the severity of the disease in patients at early stage of atherosclerosis. Collectively, the phage library-derived triabody were successfully translated into a quick immunoassay with higher affinity against a pathogenic epitope that allows not only early detection but also real-time monitoring of the disease progression to minimize the risk of atherosclerotic cardiovascular disease.

1. Introduction

Cardiovascular disease are the main cause of mortality globally, and their prevalence is increasing in current aging societies [1]. According to the World Health Organization, 17.9 million people died from such cardiovascular diseases as coronary heart disease, cerebrovascular disease, peripheral artery disease, rheumatic heart disease, congenital heart disease, deep vein thrombosis and pulmonary embolism each year, which account for 32 % of all deaths worldwide [2,3]. Basically, the pathogenesis of all cardiovascular diseases is atherosclerosis-related,

Abbreviations: ELISA, enzyme-linked immunosorbent assay; ALDH4A1, aldehyde dehydrogenase 4 family member A1; BSA, bovine serum albumin; GFP, green fluorescent protein; IgG, immunoglobulin G; OVA, ovalbumin; TMB, tetramethylbenzidine..

* Corresponding author at: College of Life Science and Technology, Xinjiang University, Urumqi 830017, China.
E-mail address: yuekang.xu@hotmail.com (Y. Xu).

[1] These authors contributed to this work equally.

https://doi.org/10.1016/j.microc.2025.115124
Received 26 May 2025; Received in revised form 28 August 2025; Accepted 29 August 2025
Available online 3 September 2025

where artery-blocking plaques form due to the accumulation of low density lipoprotein (LDL) particles [4]. These LDL particles are oxidized in the vascular walls to activate adaptive immune responses against new epitopes formed or exposed during oxidation [5–7]. The immunogenic epitopes of the LDL particles are oxidized phospholipid motif or the polypeptide chain of apolipoprotein (Apo) B-100 (ApoB100), which are the protein components of LDL [8–10].

As a lipid carrier protein, Apo can be mainly divided into ApoAI and ApoB using the ABC nomenclature [11]. While the former is the main structural protein of high-density lipoprotein cholesterol (HDL-CHO), the latter constitutes the main structural protein of LDL-CHO. Therefore, the determination of ApoB can directly reflect the level of LDL-CHO. Due to the differences in amino acid composition, ApoB can be further divided into the following subtypes: ApoB100 is a full-length protein with 4536 amino acids, while ApoB48 is a shortened version with 2152 amino acids at the N-terminus. ApoB100 is the protein constituent of very low-density lipoprotein (VLDL) and LDL, whereas ApoB48 is the protein carrying chylomicrons in the circulation [12]. Only ApoB100 serves as a critical molecular marker for atherosclerosis, with its concentration reflecting the number of lipoprotein particles that contribute to the formation of atherosclerotic plaques [13]. In contrast, ApoB48 is exclusively involved in exogenous lipid metabolism and lacks the ability to bind to low-density lipoprotein (LDL) receptors, thereby precluding its role in LDL recycling and rendering it unrelated to atherosclerosis. The ApoB100-containing LDL is responsible for the transport of endogenous cholesterol. Abnormal elevations in LDL levels represent a primary pathogenic factor in atherosclerosis, as evidenced by the significant increase in cardiovascular event risk associated with high LDL-CHO concentrations. VLDL, a triglyceride-rich particle secreted by the liver, undergoes metabolic transformation into LDL while continuously releasing ApoB100 into the circulatory system, indirectly contributing to atherosclerosis progression. The binding of ApoB100 in LDL/VLDL to the arterial wall can elicit inflammatory responses, facilitate cholesterol deposition, and promote plaque formation, with its concentration positively correlating with the severity of atherosclerosis. At the C-terminus of ApoB100 situated a short peptide, p210 with rich content of positively charged arginine and lysine residues for specific binding to negatively charged proteoglycans on the cell membrane surface via electrostatic interactions [14]. Interestingly, this p210 epitope within the ApoB100 could act as a key pathogenic antigen in atherosclerosis, as there were extensive clinical evidences for an association of IgG autoantibodies against native p210 of ApoB100 protein and a reduced risk of cardiovascular disease [6,7,15,16]. Therefore, measuring the level of this epitope should provide a more precise reflection of disease progression compared to total ApoB100 levels.

The current diagnostic methods for atherosclerosis mainly include: color ultrasound examination (to observe whether there is fatty atherosclerotic plaque in the artery), coronary angiography (to inject contrast media into the coronary artery and reveal the blood vessel shape through contrast media development to determine whether the coronary artery is narrow or atherosclerotic), X-ray examination (to see the shadow of calcinosis when the aortic node protruded upward, and the aortic shadow become widened and distorted), ultrasonic vascular examination (to determine the blood flow of the limbs arteries, kidney arteries, carotid arteries and vascular disease problems) etc. [17]. Due to the asymptomatic nature of atherosclerosis, however, early diagnose becomes impossible before the presence of plaque when atherosclerosis has entered a more advanced stage. Even in late-stage diagnosis, ELISA kits based on commercially available antibodies target entire ApoB protein. Antibodies' limited specificity and probable cross-reactivity with non-disease-associated epitopes in all ApoB proteins, including both ApoB 100 and ApoB 48 variations, significantly limit their clinical accuracy as diagnostic tools [12], let alone the fact that only ApoB 100 serves as a recognition signal for the cellular binding and internalization of LDL particles via the LDL receptor during atherogenesis.

Given the current lack of early diagnosis and urgent need for specific detection of the development of atherosclerosis, in present study we genetically engineered a triabody with three single chain of variable fragments (scFvs), all specific against the pathogenic p210 epitope in the atherosclerosis-related ApoB100, and established a rapid immunoassay to not only detect the presence but also monitor its severity in patients with atherosclerosis at various developmental stages.

2. Materials and methods

2.1. Materials

Ovalbumin (CAS: A5378), an albumin protein purified from chicken egg white, was obtained from Sigma-Aldrich. The p210 hapten (Human p210 antigen peptide of ApoB100 KTTKQSFDLSVKAQYKKNKH) were produced in Sangon (Shanghai, China). Human APOB ELISA Kit (CAS: KE00158) were bought from Proteintech (Wuhan, China). Biodragon (Suzhou, China) supplied goat anti-mouse IgG conjugated with horseradish peroxidase (IgG-HRP) (CAS: BF03001) and goat anti-rabbit IgG conjugated with horseradish peroxidase (IgG-HRP) (CAS: BF03008). Abcam (Shanghai, China) supplied native human apolipoprotein B (CAS: ab91112). All remaining materials and chemical reagents were of analytical purity and obtained from commercial suppliers.

2.2. Complete antigen preparation and animal immunization

To conjugate p210 to carrier proteins, the 1-ethyl-3-(3-dimethylaminopropyl) carbodiimide hydrochloride (EDC) method was employed [18]. The mixture was dialyzed with 0.01 M PBS (pH 7.4) after reaction period. Ultimately, the conjugated products were stored at −20 °C for subsequent usage.

Non-denaturing gel electrophoresis was employed to examine the p210-BSA/OVA conjugates, while a BCA protein concentration assay kit was utilized to measure the complete antigen's concentration. To generate high-titer antiserum, BALB/c mice and SD rats (aged 6–8 weeks) received immunizations of p210-BSA conjugates (0.1 mL, 100 μg) mixed with an equal amount of Freund's complete adjuvant for the initial dose. Subsequent immunizations were administered 8 times every two weeks interval, with an equal volume of Freund's incomplete adjuvant and dose reduced to 50 μg (0.05 mL) conjugates. The antiserum titer of immunized mice and rats' serum were assessed by indirect ELISA. The animal experiments followed guidelines provided by Anhui Normal University's Animal Experimentation Ethics Committee.

2.3. PCR amplification of the VH and VL genes and construction of phage-displayed scFv libraries

To construct an animal immune scFv library, mice and rats were sacrificed after obtaining high serum titers, and spleen cells were collected for RNA extraction. The extracted mRNA was utilized to create first-strand cDNA using reverse transcription PCR (RT-PCR) [19]. The coding sequences for the variable fragments of the heavy (VH) and light chains (VL) were then amplified from the first-strand cDNA using primary PCR. Murine universal antibody primer sequences were utilized to amplify the mouse or rat VH and VL. To assemble a scFv antibody fragment, a special sequence encode linker $(Gly_4Ser)_3$ was developed. The 45 bp DNA acts as a bridge linking VH and VL fragments, and is amplified by overlap extension-PCR (SOE-PCR), with an approximate molecular ratio of VH-linker to VL-linker approximately 1:1 [20]. With another round of PCR, the *Sfi* I and *Not* I restriction sites were introduced to either end of the scFv antibody fragment before cloning it into the phagemid vector pCANTAB-5E [21]. The product was ligated with a predigested phagemid vector and subsequently electroporated into competent *E. coli* TG1 cells. For colony quantification, 100 μL of the diluted transformed cells were plated onto 2YT-AG agar plates and incubated overnight at 37 °C. Then M13KO7 served as the helper phage to supply capsid protein during the rescue. All cultures were centrifuged

and the pellets moved to another sterile flask for phage package and cultured in 2YT-AK at 30 °C. After that the supernatants were centrifuged for 12,000 *g*, 20 min, 4 °C to obtain recombinant phage scFv antibody.

To generate human patient's scFv library, prior to extracting total RNA, the peripheral blood mononuclear cells (PBMC) from patients with atherosclerosis were obtained from the First Affiliated Hospital of Wannan Medical College. Total mRNA was isolated from PBMC using Trizol method. The isolated RNA was then reverse transcribed using the cDNA Synthesis SuperMix Kit to produce first strand cDNA. The generated cDNA was then employed as a template for amplification of the VL and VH genes using universal human antibody primers. The remaining procedures were carried out in accordance with the instructions for building an immune library.

2.4. Biopanning of phage display library

Immunotubes were coated with 2 mL of p210-OVA antigen in coating buffer (pH 9.6) at 5 μg/mL and incubated overnight at 4 °C. Following three washes with PBS, the immunotubes were blocked using PBS containing 2 % non-fat milk. Simultaneously, an uncoated immunotube was blocked with PBSM as a control. The efficiency of biopanning was enhanced by precipitating phage particles with polyethylene glycol (PEG)/NaCl on ice for 4 h, following centrifugation at 12,000 *g* for 30 min at 4 °C [20]. The phage pellet was resuspended in 2 % PBSM and incubated in a control immunotube at room temperature for an hour. Subsequently, the recombinant phage was transferred to a pre-treated immunotube. After incubating at 37 °C for 2 h, the immunotube was thoroughly washed 20 times with PBS and another 20 times with PBST (PBS containing 1 % Tween 20) to remove any unbound phages. The neutralization procedure consisted of eluted phages that had reacted with p210 using 3 mL of Gly-HCl (0.1 mol/L, pH 2.2), followed by neutralization of the elution buffer with 2 mL of Tris-HCl (1 mol/L, pH 8.0). Log-phase *E. coli* TG1 cells were infected with the eluted phages, and 10 μL aliquots of the infected bacterial suspension were plated on 2YT-AG agar (2YT medium supplemented with 100 μg/mL ampicillin and 2 % glucose). Individual colonies were isolated and clone numbers were enumerated. Totally, this biopanning process was repeated for three consecutive rounds.

2.5. Identification of the clones with higher binding specificity from the enriched clones

Enriched monoclonal cells were picked and cultured in a cell culture tube with M13KO7 for rescue, and then ELISA plate was coated with 5 μg/mL of p210-OVA antigen in pH 9.6 coating buffer (100 μL/well) overnight at 4 °C, blocked with PBSM, and washed. Phage supernatant from an M13KO7-infected clone culture was dissolved in 2 % PBSM at a 1:1 ratio, applied to the plate, and incubated at 37 °C for 2 h. After three rounds of washing with PBST and PBS, the attached phage was identified with an anti-M13 mouse monoclonal antibody diluted to 1:5000 and incubated for one hour. After washing, add 100 μL of goat anti-mouse IgG-HRP (1:5000 in block buffer) to each well and incubate for 1 h at 37 °C. The color development was performed by employing 3,3,5,5-Tetramethylbenzidine (TMB, 100 μL/well), which was stopped by adding 2 M H_2SO_4 (100 μL/well). A microplate reader was used to determine absorbance at 450 nm. Comparing the antigen well's values to the negative control's c absorbance allowed for evaluation of phage binding activity. The positive clone was selected to send to company for phagemid sequencing.

2.6. Specificity analysis of anti- p210 scFvs

BSA, OVA, ALDH4A1, OVA-p210, and MILK were used to coat 96-wellplates in triplicate (5 μg/mL; 100 μL/well) at 4 °C overnight. The plates were then blocked with 5 % PBSM [21]. Following a 2-h incubation at 37 °C, recombinant phage particles containing scFv were added, and the scFv clone was detected using mouse anti-M13 monoclonal antibody and HRP conjugated goat anti-mouse IgG polyclonal antibody at 1:5000 dilution. To stop the reaction, 100 μL of stop solution was added to each well after 15 min of incubation with TMB substrate (100 μL/well, 37 °C, dark conditions). Optical density measurements were subsequently performed at 450 nm using a microplate reader.

2.7. Epitope predication and 3D structure simulation

The mature peptide sequence and potential epitopes of p210 were further evaluated using the B-Cell Linear Epitope Prediction program on the Immune Epitope Database Analysis Resource server (http://tools.immuneepitope.org/bcell/) [22]. Meanwhile, the 3D structure of p210 (The p210 peptide along with its amino acid sequence, including the 10 amino acids preceding and following the p210 segment in ApoB100) was predicated on the basis of homology modeling using SWISS-MODEL (http://swiss.model.expasy.org/) [23].

2.8. Bioinformatic analysis of the anti-p210 scFv gene, homology modeling and molecular docking

Using BLAST, the homology among the scFv gene sequence and known murine, rattus or homo antibody genes in the GenBank/EMBL and V-Quest databases was determined. By analyzing the V-Quest IMGT (https://www.imgt.org/) [19,24], the germline origin of the VH and VL regions was identified. The database was used to align optimized complementarity determining regions (CDRs) with published crystal structures.

The 3D structural model of the scFv-A1, scFv-B2 and scFv-A12 were developed based on sequence similarity homology, SWISS-MODEL (https://swissmodel.expasy.org/) was utilized to generate a molecular model of the scFv and p210 antigen. The ZDock server was employed for rigid docking to make up the top 10 various orientations. It is an efficient molecular docking tool that uses the Fast Fourier Transform (FFT) algorithm to efficiently filter out potential interaction patterns and is important for understanding the mechanism of binding between antigen antibody molecules [25]. PyMOL was used to calculate the intermolecular spatial distance for docking with high ZDock scores and generate graphical molecular docking images.

2.9. Generation and expression of the MBP fusion antibodies

Following sequencing of the positive scFv clone with strongest binding activity, gene-specific primers were constructed to amplify the corresponding scFv. The pMAL-c2x vector had been employed for constructing vectors for gene expression containing the scFv-A1, scFv-B2, and scFv-A12 proteins fused to MBP tags. The expression of the scFv was achieved through the transformation of the recombinant pMAL-c2x-scFv (A1/B2/A12) plasmids into *E. coli* TB1 via electroporation. Once the LB culture achieved an OD600 of 0.8, the fused protein was expressed by induction with 1 mM IPTG (isopropyl β-D-1-thiogalactopyranoside) at 16 °C for a duration of 16 h. Subsequently, the cell pellets were harvested through centrifugation at 4 °C.

2.10. Purification and binding activity test for anti- p210 antibodies

The recombinant anti-p210 scFv was purified by MBP-affinity chromatography, and the resulting protein fractions were analyzed using SDS-PAGE to assess purity. The activity of purified scFv products was determined using indirect ELISA. The 96-well plates were coated with serially diluted OVA-p210 antigen and kept overnight at 4 °C. After that, the purified, fused scFv proteins, which varied in concentration, were added to reaction wells to incubate for a period of 2 h at 37 °C after blocking process. In the following of the reaction, an anti-MBP tag antibody (1:1000 dilution) was added to the reaction wells and a goat

anti-mouse IgG antibody conjugated HRP at 1:5000 was utilized to amplify the chromogenic signal. The enzyme process was performed with tetramethylbenzidine (TMB) as the substrate, and the color formation halted by the addition of 2 M H_2SO_4. The measurement of the absorbances at 450 nm was conducted using a microplate reader.

2.11. Identification of anti- p210 antibodies

In order to ascertain the binding affinity of the expressed anti-p210 scFv antibody (MBP-linker-scFv), an indirect ELISA checkerboard assay was conducted. In summary, within ELISA plates, the p210 epitope was serially diluted and reacted with the different concentrations of expressed scFv. The K_{aff} formulathat was employed was $Kaff = \frac{n-1}{2\times(n[Ab]t-[Ab])}$ [20,26,27], where K_{aff} refers to the affinity constant; n is the proportionality coefficient associated with antigen coating concentration; [Abt] and [Ab] correspond to the antibody concentrations at the half-maximal absorbance point. This approach is widely used for quantifying affinity constants between antibodies and immobilized antigens due to its operational simplicity and reproducibility [18,21,22,26–33].

To determine the specificity of the anti-p210 scFvs (MBP-Linker-scFv A12/B2/A1), Different protein antigens, including BSA-p210, OVA-p210, ALDH4A1, tetranectin (TN), GFP, BSA, OVA and PBSM were coated in 96-well ELISA plates (5 μg/mL). The remaining ELISA processes were identical to those described above in 2.10.

Meanwhile, to assess the antibody inhibitory ability to p210, indirect competitive ELISA (ic-ELISA) was conducted [34]. The competition antigen was the standard p210 epitope synthesized from company to react with the MBP-linker-scFv antibody at 37 °C incubation for 2 h, which were followed by the other ELISA steps mentioned earlier. Origin 8.0 was employed to show the typical calibration curve and linear portion of the standard curve, and B/B0 determined by calculating it over the p210 concentration.

2.12. Construction of anti-p210 triabody

In order to improve recombinant antibody binding activity and the stability of antigen-antibody complex, scFv-A1, B2 and A12 encoding gene was fused and linked together by SOE PCR and constructed into pMAL-c2x expression vector. For expression of triabody, the plasmids were transformed into *E coli* TB1 strain. Transformed bacterium were growing at 37 °C for amplification in shake flasks and induced by IPTG (Isopropyl β-D-thiogalactopyranoside, 1 mM) for overnight at 16 °C. Following MBP tag affinity chromatography, the trimeric scFv of MBP fusion expression is purified and identified.

2.13. Identification of reactive anti-p210 triabody with high affinity

After the purification process, the binding activity of assembled trimeric scFv was measured using indirect ELISA. The affinity, specificity and inhibition of triabody were performed as the above in Section 2.11. To confirm triabody binding capacity to total ApoB100, western blotting was performed as follows. The human naïve Apolipoprotein B 100 (ab91112) antigen was transferred onto a nitrocellulose (NC) membrane from a SDS-PAGE gel, and the triabody was utilized as the primary antibody to react with the antigen. Subsequently, an anti-MBP tag antibody was incorporated into the blocking buffer as the secondary antibody, and a goat anti-mouse IgG-HRP antibody was utilized eventually. The signals were observed using enhanced chemiluminescence (ECL) for reaction.

2.14. Generation of PAbs against apoB100

To generate polyclonal antibodies (PAb), female New Zealand rabbits were immunized with human naïve apolipoprotein B 100 as described in Section 2.2. The antibody titration of the antisera was measured by indirect ELISA, briefly, native ApoB100 was immobilized onto ELISA plates and blocked overnight with PBS-containing milk. Serial dilutions of serum (from 1:1000 to 1:512000) were then applied. Following incubation, an HRP-conjugated goat anti-rabbit IgG secondary antibody was added at a dilution of 1:5000. Enzymatic activity was detected using tetramethylbenzidine (TMB) as the substrate. The colorimetric reaction was stopped after 15 min with 2 M H_2SO_4, and absorbance was measured at 450 nm using a Bio-tek microplate reader.

2.15. Development of sandwich ELISA based on anti-p210 triabody

The sandwich ELISA was developed using triabody as the capture antibody and pAb as the detection antibody. Firstlly, triabody or monomeric scFv dissolved in 0.01 M PBS (5 μg/mL) was coated on ELISA plates. Following blocking and washing steps, various concentrations of human naïve Apolipoprotein B-100 (250,000, 125000, 62500, 31250, 15625, 7812.5, 3906.25, 1953.125, 976.5625, 488.28125, 244.140625, and 122.0703 ng/mL) and PBSM (blank, without ApoB100 antigen) were incubated in consecutive wells. The theoretical concentration of the p210 epitope was determined by multiplying the initial concentration of the ApoB100 standard by the molecular weight ratio of the p210 epitope (2.37 kDa) to the full-length ApoB100 protein (515 kDa). This ratio equates to 1/217, meaning the resulting epitope concentration amounts to 1/217th of the original ApoB100 input. Following the incubation and washing step, rabbit anti-ApoB100 polyclonal antibody (1:1000) were used across the row. After a final washing step, the reaction was completed by adding HRP-tagged anti-rabbit secondary antibody (1:4000) and TMB substrate for color development. Solution containing sulfuric acid (2 M H_2SO_4) was used to stop reaction and the color intensity proportional to the quantity of p210 epitope measured at 450 nm. A statistical approach was used to calculate the limit of detection (LOD = Mean $_{blank}$ + 2 SD $_{blank}$) [35].

2.16. Blood samples detection based on anti-p210 triabody

The repeatability, sample recovery, and accuracy of sandwich ELISA were determined by using both intra- and inter-assays. The mean recovery of sandwich ELISA was determined by adding varying amounts of p210 peptide to samples with no residual p210 antigen. The average recovery and coefficient of variation values (CV%, ratio of standard deviation to mean) of spiked samples with p210 concentrations (100, 200, 300, 400, and 500 ng/mL) were measured for four times in both intra- and inter-assays.

Blood samples were collected from the First Affiliated Hospital of Wannan Medical College for atherosclerosis patients and healthy controls. The entire blood was centrifuged at 2000 *g* for 15 min, and the top layer of transparent plasma (without blood cells) was extracted [18]. After mixing 15 μL of plasma with 285 μL of PBSM (blocking buffer PBS-MILK), 100 μL of the mixture was transferred to ELISA plates that were triabody pre-coated and PBSM blocked to incubate for 1 h. Following washing with PBST and PBS, the rabbit polyclonal antibodies (detection antibody) at 1:5000 was added to PBSM for reaction. The subsequent steps were carried out as indicated in Section 2.14.

To confirm the detection results of scFv, commercial Human APOB ELISA Kit was used to detect and quantify ApoB100 protein levels of plasma. The detection process was carried out exactly in accordance with the instruction manual that was provided with the commercial ELISA kit.

2.17. Statistical analysis

At least three experiments were performed, and the data is presented as the mean +/− standard deviation (SD), with n representing the number of experiment times. In the case of uncertainty measures (standard errors, root mean square errors, relative prediction errors) and

also parameters derived from uncertainties (detection limit, quantitation limit), they should be reported with one or at most two significant figs. [36]. ANOVA was used to determine statistical differences among more than two groups that had a normal distribution and met variance homogeneity [37,38]. All data was analyzed using Prism Software, and *P* values less than 0.05 were deemed statistically significant.

3. Results

3.1. Complete antigen and animal immunization

Due to p210 is a hapten inside the ApoB100 protein that has only 20 amino acids in length, conjugation of the carrier protein is necessary to efficiently generate immune responses in rodents for antibody production. Therefore, the carbodiimide crosslinker EDC was employed to conjugate the human p210 peptides to carrier protein BSA or OVA, as p210-BSA or p210-OVA respectively, and the results were showed in Fig. S1. When performing non-denaturing gel electrophoresis, the conjugates with higher molecular weight migrated more slowly than carrier proteins only did, suggesting successful conjugation of carrier proteins to the p210. Non-denaturing agarose gel electrophoresis was employed to characterize the cross-linked antigens based on their molecular weight and charge. The primary objective was to highlight the differential migration velocities of the antigen before and after the cross-linking reaction [27,39–42]. Following eight subcutaneous immunizations with the p210-BSA immunogen, administered at two-week intervals, antiserum obtained from inoculated mice and rats was analyzed using an indirect ELISA to ascertain the antibody titer in vivo against the detection antigen, p210-OVA. Compared to the negative control (pre-immune serum), the p210-BSA immunized serum reacted with p210-OVA in a dosage-dependent manner. However, it did not respond with OVA, indicating the production in vivo of polyclonal antibodies against p210 epitope (Fig. S2A and Fig. S3A). Furthermore, the immunized mouse had anti-p210 titer about 1:3200 while the titer in immunized rat reached 1:6400 (Fig. S2A; Fig. S3A). Notably, the antiserum titer of SD rat was approximately double that of BALB/c mice, further confirming that the complete antigen was successfully prepared and animal immunization works effectively in different species.

3.2. ScFv libraries construction and bio-panning

The first chain cDNA was produced using an RT-PCR kit and total RNA as template from the splenocytes of the immunized animals (BALB/c mice and SD rats) or patient's peripheral blood mononuclear cells (PBMC). The cDNA templates mentioned above was used for VH and VL gene amplification, and the lengths of the VH and VL DNA fragments were approximately 350 bp and 320 bp, respectively (Fig. S2B and Fig. S3B). For homo antibody gene library, in the initial PCR, VH PCR products are approximately 380 bp in length, while kappa or lambda light chains are approximately 650 bp. The second PCR appears to be similar to the first PCR, but the length of the VH PCR products is around 400 bp due to the addition of restriction sites, whereas the length of kappa or lambda VL is approximately 400 bp as shown in Fig.S4B. A SOE-PCR reaction was used to assemble the VH, VL, and linker genes into a complete scFv gene for three different derives, and the assembled scFv fragments all had an approximate size of 750 bp (Figs.S2-4C), which were then digested and inserted into the phagemid pCANTAB-5E. After transformation into *E. coli* TG1, the recombinant phagemids were verified by bacteriophage PCR to determine the accuracy and insertion rate of the scFvs. The percentage of murine, rattus or homo antibody genes that were successfully inserted was 82 %, 86 % and 85 % respectively (Figs. S5-7 A), indicating that high-quality antibody libraries had been generated. With the rescue of helper phage M13KO7, the displayed scFv libraries were employed to 1.8×10^8 pfu/mL (mouse immune library, Fig. S5C), 3.0×10^8 pfu/mL (rat immune library, Fig. S6C) or 1.6×10^8 pfu/mL (human patient's library, Fig. S7C), and the elution of these phage libraries were shown in Figs. S5—7C. Following three rounds of bio-panning, the eluted phage clones were all kept at a level of around 10^6 pfu/mL, suggesting that more specific scFvs were attached to the p210 antigen on the immunotubes during bio-panning and enrichment (Figs. S5—7B). Then, several clones were randomly selected and screened by phage ELISA and sequenced. Furthermore, the clones of highest affinity that displaying the strongest binding activity (Fig. 1) were selected and named as scFv-A12 (murine scFv library), scFv-B2 (rattus scFv library), or scFv-A1 (homo scFv library) respectively. To identify the specificity of the scFv-A12, scFv-B2, and scFv-A1, various antigens including OVA, BSA, ALDH4A1, p210-OVA, and skimmed milk (PBSM) were assayed in triplicates by indirect ELISA. As shown in Fig. S8, the phage antibodies scFv-M-A12, scFv-R-B2, and scFv-H-A1 specifically recognized the p210 antigen without any cross-reactivity to the other related antigens.

3.3. Bioinformation of the scFv and evaluation of epitope binding pattern

BLAST was used to determine homology between the scFv gene sequence and any reported antibody genes from the GenBank and V-Quest databases. The scFv clone sequence (Fig.S9) was analyzed using V-Quest IMGT (International Immunogenetics Information System [http://www.imgt.org]) to identify the germline origin of the VH and VL regions. Fig. S10 shows IMGT "collier de perle" graphical two-dimensional (2-D) representations of the three scFvs.

The antigenic sites on the p210 were identified utilizing the Bepipred B-cell linear epitope prediction program. As demonstrated in Fig. S11A, this antigen has a single major epitope at positions 5–16 of the protein sequence. Therefore, we predict that the major epitope that the antibodies bind is likely to fall in this region.

3.4. Homology modeling and molecular docking

Since the molecular docking is an effective method to study the molecular interaction and recognition of antibody-antigen [43], the 3D homology modeling of the scFv domain and ApoB100 p210 epitope were carried out by SWISS-MODEL and docked by ZDock online server. As were demonstrated in Fig. S12, it was evident that the conformation of p210 epitope was inside the murine scFv-M-A12 binding cavity. Furthermore, visualizing the interactions between the antigen and the antibody complex showed that hydrogen bonds were formed between the residues of murine scFv HCDR3 ARG100 and residue Vla11 of p210 epitope (bond length: 2.8 Å); HCDR3 Gly102 and Vla11 (2.0 Å); HCDR3 Asn103 and SER10 (2.5 Å); HCDR3 Gly105 and SER10 (2.0 Å); HCDR3 ASN106 and Asp8 (2.9 Å); HCDR3 Ser107 and SER10 (2.9 Å); HCDR3 Tyr110 and Ala13 (2.8 Å); LCDR3 TRP230 and Phe7 (2.9 Å) (Fig. S12).

Also shown in Fig. S13, the conformation of p210 epitope was inside the binding pocket of the rattus scFv-R-B2, which was found in the HCDR3 loop regions of the antibody, with residue PHE83 forming hydrogen bond (2.5 Å) with p210 residue 15YTR. HCDR3 HIS94, and residue TYR95 forming hydrogen bond with p210 at SER6 and Gln5 (2.70 and 3.20 Å). Collectively, the results demonstrated that these three hydrogen bonds were the main sensitive and specific binding forces in antibody recognition [21] [43].

For homo scFv-H-A1, residues Arg95 of HCDR3 and Asp8 (2.0 Å), TYR102 and Gln14 (3.0 Å) of p210 epitope establish hydrogen bonds. The HCDR3 residue LEU101 interacted with the two epitopes (SER10 and LYS12 animo acid) of p210 via hydrogen bond of 2.90 Å and 3.20 Å distance, which play an important role in the antibody-antigen interaction (Fig. S14). These three HCDR3 residues interacted with the p210 epitope via four hydrogen bonds to maintain antigen-antibody complex conformation [44].

Among the three dimensional visualization of the antigen-antibody complex, the residues involved in hydrogen bonding are entirely located within the CDRs of the scFvs (Fig. S11B). The formation of these hydrogen bonds enhances the stability and specificity of the antigen-

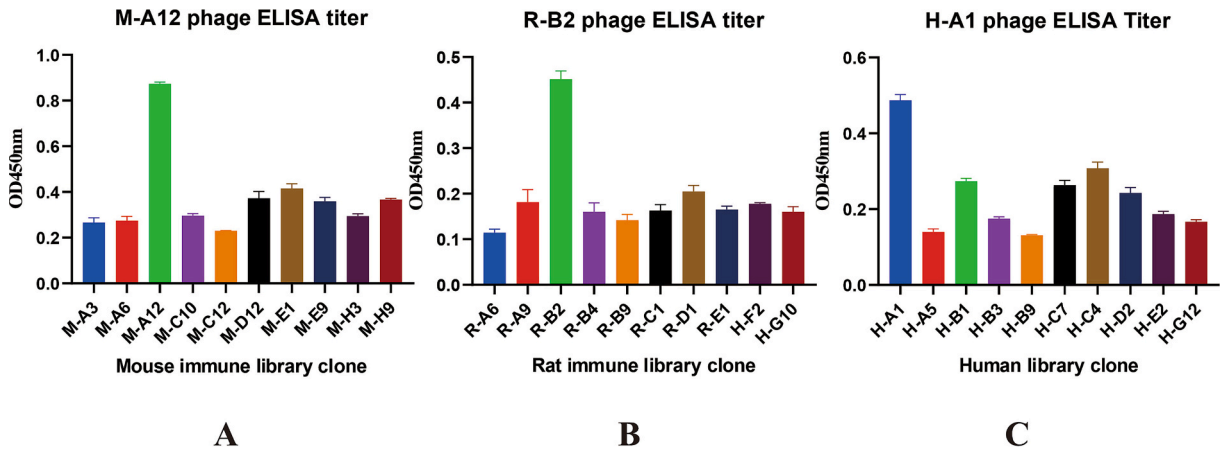

Fig. 1. The phage ELISA assay of the selected scFv clones in phage libraries of various species. Of ten positive clones obtained in each library, one clone (scFv-M-A12, scFv-R-B2, scFv-H-A1) with the highest affinity was selected for further study in (A), (B) and (C).

antibody complex [45].

3.5. Soluble expression and determination of the scFvs

Considering the solubilization-promoting effect of maltose-binding protein (MBP) tag on its linked protein [34], the fusion proteins MBP-linker-scFv (namely MBP-linker-A1, MBP-linker-B2, and MBP-linker-A12) were produced in *E. coli* TB1 cells, isolated using MBP-affinity chromatography, and subsequently analyzed by SDS-PAGE. As shown in Fig. S15, the molecular mass of the MBP control was approximately 50 kDa, while that of each MBP-linker-scFv fusion protein increased to around 70 kDa. To preserve the structural and functional integrity of the recombinant scFvs, affinity purification was carried out under mild conditions following bacterial induction, resulting in protein preparations with purities exceeding 90 % (Fig. 2).

Furthermore, in order to prove whether the scFvs conform to favorable characteristics of antibodies, indirect ELISA was carried out to validate their specificity, affinity and inhibition towards the p210 antigen. As illustrated in Fig. S19, the purified M-A12, R-B2 and H-A1 were all exclusively reactive with p210 antigen, but not with their carrier proteins, OVA, BSA or other proteins, such as MILK, TN, ALDH4A1 and GFP. Meanwhile, indirect ELISA was carried out to assay the affinity of scFvs and the affinity constant of homo scFv-H-A1, rattus scFv-R-B2, and murine scFv-M-A12 were 1.05×10^8 L/mol, 1.34×10^7 L/mol, and 2.19×10^8 L/mol respectively (Fig. S20), all belonging to high affinity antibody (affinity among10^7 to 10^{12} L/mol was generally accepted as high). The optimal concentrations for coating p210-OVA antigen and the working dilutions of scFvs used in ic-ELISA were established through checkerboard titration. As summarized in Fig.S16–18 and Fig.S23, the coating concentrations yielding a target absorbance of approximately 1.0 [18]—were determined to be 5 μg/mL for scFv-A12, 0.625 μg/mL for scFv-B2, 5 μg/mL for scFv-A1, and 5 μg/mL for the triabody. These optimized antigen levels were subsequently employed in all ic-ELISA coating steps. A standard inhibition curve for the ic-ELISA of the p210 epitope was generated by incubating purified anti-p210 MBP-linker-scFv fusion proteins with varying concentrations of competing p210 peptide (Fig. S21). The correlation between p210 concentration and inhibition rate was evaluated using Origin 8.0 software. The calculated half-maximal inhibitory concentration (IC_{50}) values for p210 binding to scFv-H-A1, scFv-R-B2, and scFv-M-A12 were 0.576 μg/mL, 0.88 μg/mL, and 1.079 μg/mL, respectively. These results demonstrate that the recombinantly produced and purified MBP-linker-scFv proteins are suitable for use as detection antibodies against the p210 peptide.

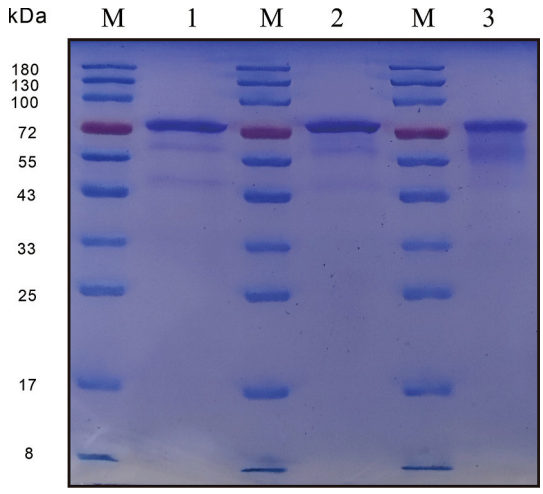

Fig. 2. SDS-PAGE of purified MBP fused scFvs. Three distinct protein bands at 70 kDa, indicate effective purification from *E coil* lysis product for each scFv. M: protein marker, lane 1: MBP-linker-H-A1-scFv, lane 2: MBP-linker-R-B2-scFv, lane 3: MBP-linker-M-A12-scFv.

3.6. Identification of anti-p210 triabody and development of sandwich ELISA

Since the pathogenic p210 epitope is extremely low in circulation, and engineering monovalent scFv into multivalent molecules such as diabody, triabody or larger aggregates can significantly enhanced their functional affinity and specificity to the targeted antigen [46,47], we thereby tried to increase the functional affinity of our detecting reagent by incorporating more scFvs. After amplification of scFv-H-A1, scFv-R-B2 and scFv-M-A12 genes by PCR, scFv-A1 and scFv-B2 was firstly overlapped as a diabody, then scFv-A12 and the diabody were assembled to become trimeric scFv fragments which were amplified by SOE-PCR using a flexible $(G_4S)_3$ DNA linker gene. Fig. S22A shows the PCR identification of the triabody, with about 2400 bp of the predicted trimeric scFv band amplified successfully. Furthermore, the scFv genes of triabody was inserted into the pMAL-c2x expression vector containing MBP gene, and expressed by IPTG (Isopropyl β-D-thiogalactopyranoside) induction. The scFv protein (Fig. 3) was expressed and purified using affinity chromatography and analyzed using SDS-PAGE (Figs. S22B-C).

The affinity constant of the anti-p210 triabody was assessed via the protocol described as monomeric scFvs above. The result was illustrated in Fig. S24, and the affinity constant of trimeric scFv was 7.89×10^8 L/mol, which is 2.5 times higher than that of the highest monomeric scFv-A12 among the three differently derived scFvs. To validate the binding

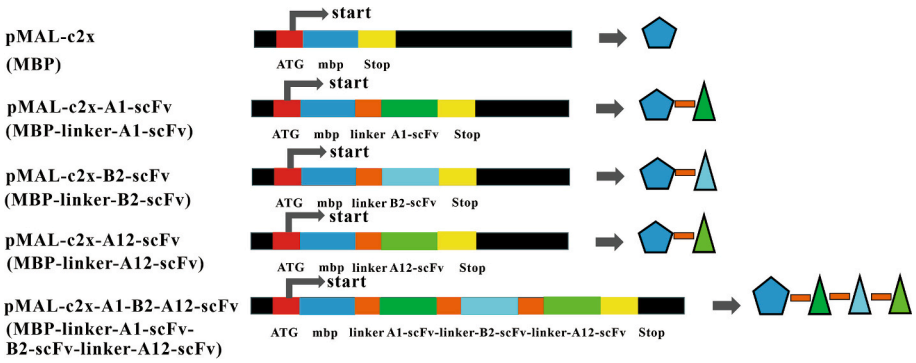

Fig. 3. The schematic profiles of expression vector construction and scFv fusion formats against p210 epitope for MBP, MBP-linker-A1-scFv, MBP-linker-B2-scFv, MBP-linker-A12-scFv and MBP-linker-A1-scFv-linker-B2-scFv-linker-A12-scFv. ATG, start codon; MBP, maltose binding protein; Linker, $(G_4S)_3$ linker chain; scFv: single chain fragment; Stop, stop codon.

activity of the triabody to native human ApoB100 entire protein, western blotting was done, and a clear band at 500 kDa was shown following ECL chemiluminescence and graphic (Fig. S25), indicating that the trimeric scFvs effectively binding to the human naïve ApoB100 antigen immobilized on the NC membrane. To identify the specificity of triabody, the purified trimeric scFvs were assayed by iELISA and found only reactive with p210 peptide, with no cross-reactivity to other antigens (Fig. S26).

Finally, ic-ELISA was performed to develop a standard curve (Fig. S27). The inhibition data were analyzed using Origin 8.0 software. The half-maximal inhibitory concentration (IC_{50}) of the triabody for p210 binding was determined to be 0.209 μg/mL, which was significantly lower than those of the monovalent antibody fragments (H-A1 IC_{50} = 0.576 μg/mL, M-B2 IC_{50} = 0.88 μg/mL, M-A12 IC_{50} = 1.079 μg/mL). Additionally, the IC_{50} value for the triabody was found to be 0.209 μg/mL, with its half maximal inhibitory concentration against the p210 antigen being approximately half that of the most competitive monomeric antibody, H-A1-scFv, among the three scFvs. These findings indicated that the triabody probably exhibited superior inhibitory capability against the p210 and could detect the pathogenic epitope of p210 within a lower concentration range effectively. Collectively, the above result demonstrated that the triabody developed had higher affinity and binding activity, and might be suitable for quantitative detection of p210 antigen.

3.7. Standard curve and spiked samples determination

To establish a standard curve for analyzing the p210 pathogenic epitope using sandwich ELISA, the triabody was coated on the ELISA plates that bind three p210 epitopes at once that suited on the surfaces of ApoB100 antigens. After attaining a satisfied titer of 1: 256,000, polyclonal detecting antibodies were purified from rabbit antiserum (Fig. S28). The sandwich ELISA standard curve was plotted by p210 at dosages ranging from 1152 to 0.56 ng/mL and fitted using a nonlinear logistic curve. Fig. 4A depicts the OD values at various p210 concentrations. From the typical calibration curve illustrated by plotting OD450nm against p210 concentration, the equation of the logistic curve was $y = 3609.813 + [(0.28706–3609.813)/(1 + x/1.57498)^{0.69479}]$, with a correlation coefficient (R^2) of 0.9804. The Limit of detection (LOD) of the ELISA was 28.5 ng/mL, and the linear equation is $y = 0.36076 \times -0.2322$, with a correlation coefficient (R^2) of 0.983 and the linear range between 36 and 576 ng/mL (Fig. 4B).

To evaluate the detection performance of the engineered triabody in a sandwich immunoassay format relative to monomeric single-chain variable fragments (scFvs), we conducted additional sandwich ELISAs for scFv-M-A12, scFv-R-B2, and scFv-H-A1, as provided in the Supplementary Materials (Fig. S29–31). The linear detection ranges for these monomeric scFvs ranged from 72 to 1152 ng/mL, which was higher than that of the triabody (36–576 ng/mL). However, the minimum detection limits for the monomeric scFvs (41.2 ng/mL, 58.8 ng/mL, and 34.4 ng/mL, respectively) were all higher than that of the triabody (28.5 ng/mL). These results indicate that the trivalent antibody exhibits improved

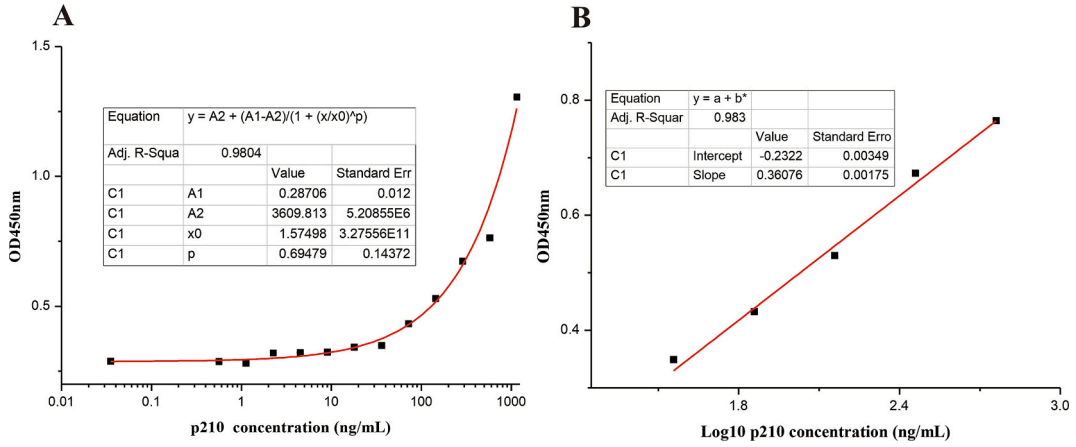

Fig. 4. Typical curves of sandwich ELISA for the detection of p210 epitope. (A) Standard calibration curve plotting OD450nm against p210 concentration, the equation of the logistic curve was $y = 3609.813 + [(0.28706–3609.813)/(1 + x/1.57498)^{0.69479}]$, with a correlation coefficient (R^2) of 0.9804. The limit of detection (LOD) was 28.5 ng/mL. (B) Linear range graph conserved from (A). The equation is $y = 0.36076 \times -0.2322$, with a correlation coefficient (R^2) of 0.983. The range of linear detection for p210 pathogenic epitope was 36–576 ng/mL.

immunoassay sensitivity over its monomeric counterparts. To analyze the recovery of detection and coefficiency of variation (CV), standard curves of sandwich ELISA were performed, with the standard p210 epitope added to the diluted buffer at various concentrations (100, 200, 300, 400, 500 ng/mL). The average recoveries within and between batches were (88.4 ± 3.0)% and (85.5 ± 5.2)%, respectively, with an average CV ranged from 4.1 % to 6.1 % (Table 1).

3.8. Detection of p210 by sandwich ELISA in clinical plasma samples

Following the validation of the sandwich ELISA as a viable detection method with adequate sensitivity and recovery in spiked samples, we investigated its use for blood detection in clinical instances of atherosclerosis. Blood samples were gathered from patients at Wannan Medical College's First Affiliated Hospital, while healthy persons served as controls. First, we discovered that there was a good linear association between ApoB100 concentrations (measured by commercial kits) and p210 epitope levels (detected by our triabody) in the patient's plasma (Fig. 5A), indicating the accuracy of our assay (Table S1 and Table S2). Furthermore, we employed the trimeric antibody to evaluate the p210 levels in plasma and discovered that the p210 epitope concentration in the plasma of twelve patients with atherosclerosis was all higher than that of healthy controls (Fig. 5B), and the average value of which was calculated to be 4.80 ± 0.92 μg/mL, suggesting that the amount of atherosclerosis-inducing p210 epitope assessed by the triabody can accurately indicate disease severity and be normalized. The patient's values were found to be higher than those of the control group, which indicated the possibility of atherosclerosis. Overall, these findings suggested that the sandwich ELISA approach based on the trimeric scFv established in this work can be used to detect atherosclerosis cases in clinical settings not only accurately, but also quantitatively.

4. Discussion and conclusion

Current clinical diagnostic methods for atherosclerosis primarily encompass laboratory tests, electrocardiogram assessments, ultrasound evaluations, and imaging analyses, among others [17]. These techniques, however, necessitate extensive medical infrastructure and specialized personnel. Moreover, the pathological changes associated with atherosclerosis remain asymptomatic during the early stages, which only manifest as significant clinical symptoms when vascular stenosis or blood flow obstruction occurs in the later stages, and the condition often becomes irreversible. Consequently, there is an urgent need for a comprehensive set of effective early diagnostic tools and post-treatment monitoring strategies in this field.

Measurement of atherosclerosis-related protein levels in the circulation provides a good way to diagnose and monitor the disease progression. Currently, there are two primary types of ApoB detection reagents available in the market. One is designed to detect total ApoB protein, such as the commercial kit from Abcam (Human Apolipoprotein B ELISA Kit, Catalog No. ab108807), and the other is made to measure ApoB100, exemplified by the Human APOB ELISA Kit (CAS: KE00158, provided by Proteintech, Wuhan, China). Unfortunately, none of them are specifically targeted against pathogenic epitopes, as total ApoB contain atherosclerosis-unrelated lipid protein ApoB48 (chylomicrons), and even atheroslcerlosis-related ApoB100 (LDL/VLDL) includes a lot of nonpathogenic epitopes. As a result, commercial kits may cross-react with a wide range of common epitopes in healthy individuals.

In the present research, three scFvs were effectively produced using phage display technology, with highly specific and affinity to p210 epitope in the atherosclerosis-associated autoantigen ApoB100 and no cross-reaction with other proteins in plasma or serum. Moreover, a sandwich ELISA with triabody assembled by the three monomeric scFvs was established with an LOD of 28.5 ng/mL for the p210 epitope. Additionally, the established sandwich ELISA method can be used to examine serum or plasma with a wide linear detection range 36–576 ng/mL. Notably, the triabody's quantification of the p210 epitope in patient plasma correlated to disease severity. To the best of our knowledge, immunoassays developed based on genetically engineered antibody for p210 pathogenic epitope quantitative analysis in plasma samples have not been reported. Therefore, a feasible immunoassay based on higher-affinity triabody was developed for the first time to evaluate the pathogenic epitope contents in human plasma for the diagnosis of atherosclerosis.

Following engineering three monovalent antibodies into trivalent forms, the affinity of our tribody was approximately 2.5 times higher than that of the original monomeric scFv with the highest affinity, while the IC_{50} for antigen inhibition was approximately two-fold lower than that of the most competitive monomeric antibody among the three scFvs. The underlying mechanisms are as follows: Firstly, multivalent antibodies possess multiple binding sites capable of simultaneously interacting with multiple antigenic epitopes. By linking monovalent fragments such as Fab or scFv into multimers, the number of binding sites is increased, thereby enhancing the overall binding strength of the antigen-antibody complex. Secondly, even when individual binding sites exhibit low affinity, the combined action of multiple sites binding to different epitopes (or multiple copies of the same epitope) results in a statistically significant enhancement of overall binding strength, thus improving overall affinity. Last but not least, multivalent antibodies better accommodate the spatial distribution of antigens, reducing the likelihood of dissociation of antigen-antibody complexes and enhancing binding stability. Simultaneous separation of multiple sites requires all interactions to break concurrently, which is statistically improbable. Consequently, even if the affinity of a single antibody is relatively low, the overall dissociation rate is still substantially low.

In contrast to the traditional monoclonal antibodies secreted by hybridomas that can't be manipulated genetically [23], antibody genes in the triabody scFvs from phagemid were cloned into high-yield expression vectors and transformed into the host cell to obtain recombinant super antibodies, therefore, their production is under strict

Table 1
Recovery and coefficiency of variation detection in spiked samples with p210 ($n = 4$).

Spiked		Intra-assay				Inter-assay		
conventration		Measured	Recovery	CV		Measured	Recovery	CV
(ng/mL)	n	(ng/mL)	(%)	(%)	n	(ng/mL)	(%)	(%)
100	4	82.85 ± 6.03	82.9 ± 6.0	7.3	4	84.01 ± 7.07	84.0 ± 7.1	8.4
200	4	157.01 ± 6.00	78.5 ± 3.0	3.8	4	153.91 ± 11.18	77.0 ± 5.6	7.3
300	4	284.53 ± 8.22	94.8 ± 2.7	2. 9	4	283.80 ± 16.90	94.6 ± 5.6	6.0
400	4	369.48 ± 15.02	92.4 ± 0.6	3.8	4	339.29 ± 15.24	84.8 ± 3.8	4.5
500	4	467.57 ± 12.30	93.5 ± 2.5	2.6	4	435.75 ± 20.12	87.2 ± 4.0	4.6
Average			88.4 ± 3.0	4.1			85.5 ± 5.2	6.1

Recovery = (detection concentration / spiked concentration) *100 %.
CV = (Standard Deviation/mean) *100 %.
Intra-assay variation was determined by four replicates of each spiked level on the first day.
Inter-assay variation was determined in independent days (4 times).

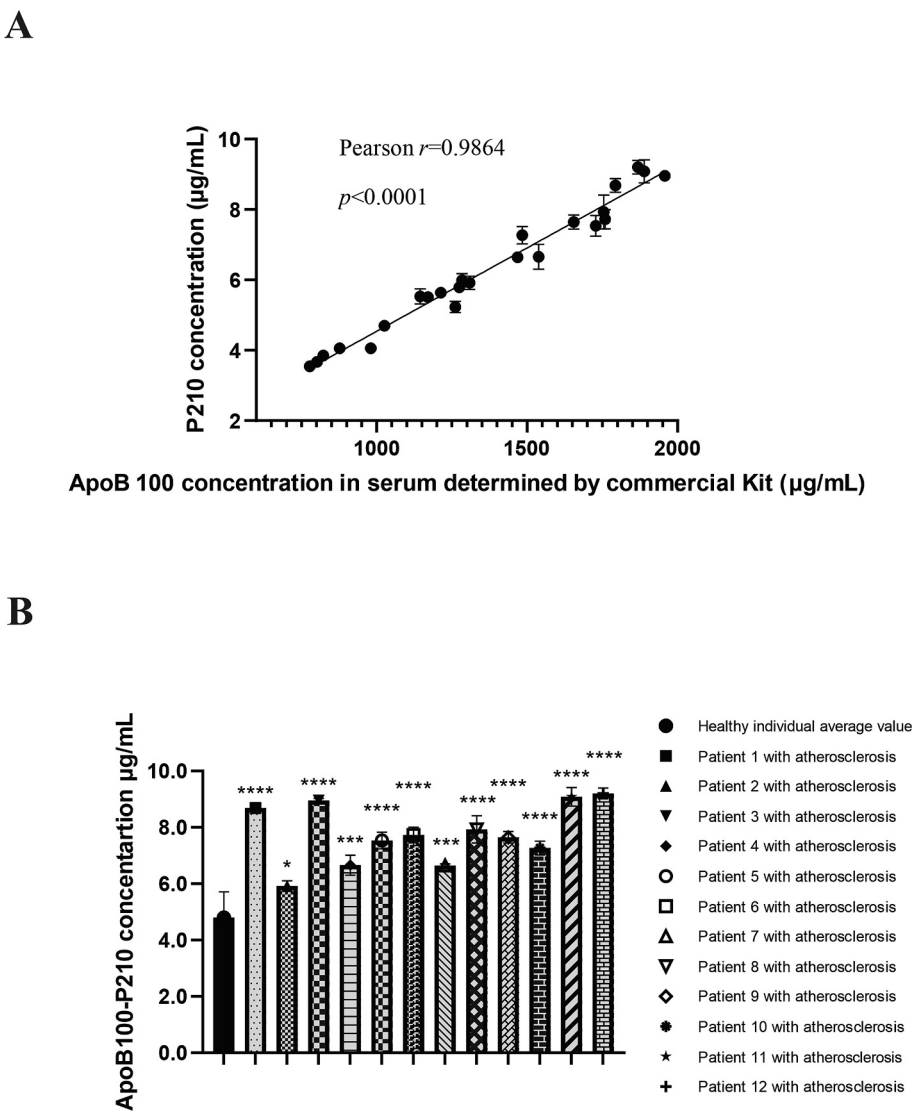

Fig. 5. Plasma p210 concentrations between healthy individuals and patients with atherosclerosis. (A) The ApoB100 concentration assessed by commercial kits corresponds to the p210 levels found by trimeric scFv in patients with atherosclerosis. Pearson $r = 0.9864$, Data are mean ± SD. **** $P < 0.0001$. (B) The healthy control value of p210 is 4.80 ± 0.92 ng/mL. However, all individuals with atherosclerosis have significantly higher levels than this normal control value. The error bar represents the standard deviation (SD) for four repetitions. The means of healthy persons and patients with atherosclerosis were compared applying one-way ANOVA. **** P < 0.0001, *** $P < 0.001$, ** $P < 0.01$. ANOVA, analysis of variance.

control and reliable. The inter-batch consistency of the recombinant antibodies is very high, and can overcome the limitations of any hybridoma antibody production methods like low repeatability and genetic drift, which makes it possible to target highly difficult targets such as toxins, nucleotides and membrane-binding proteins, providing a diagnostic progression characterized by high specificity and sensitivity disease monitoring. Furthermore, generated recombinant antibody could ensure a long-term stable supply, and achieve high-throughput production in vitro.

In recent decades, significant advancements have been made in the field of molecular diagnostics and immunological detection. Among these developments, molecular immunoassay has emerged as the most prevalent technique over the past decade, owing to its high diagnostic specificity. The triabody test devised in this work differs fundamentally from those utilized in common ELISA Kits. In the traditional sandwich ELISA, usually capture antibody is divalent and can react with two epitopes, while triabody is trivalent to three antigen determinants (epitopes). This means that antibodies of the same quality can bind to more antigens and increase the rate of antigen-binding efficiency in immunoassay. Since p210 in the ApoB100 is a linear epitope, our trimeric scFvs that targets linear epitope is a better option for clinical diagnostics than antibodies that target only conformational epitopes when clinical samples more often than not, become denatured in normal storage conditions, or by other variables that interfere with conformational epitopes. Additionally, the p210 residue motif selected for the triabody binding is a crucial pathogenic epitope of the ApoB100 antoantigen, whose level indicates the serum concentration of atherogenic lipoproteins. [48]. Since the p210 fragment is a causative factor in the illness and is unique to atherosclerosis start, the amount of its binding to triabody indicates disease severity. Altogether, the triabody-based sandwich ELISA approach has proven to be accurate in both clinical diagnosis and disease severity evaluation for atherosclerosis. This approach has the potential to serve as an effective guide for immunoassays for other diseases.

Bioethics statement:

Healthy controls and patients with atherosclerosis were both subjected to blood sampling at the First Affiliated Hospital of Wannan Medical College (Wuhu, China). The collection of blood samples was

approved by the Human Ethics Committee of the First Affiliated Hospital of Wannan Medical College. The Human Ethics Committee of Anhui Normal University reviewed and approved the study (AHNU-ET2023029). Representative 24 human individuals' (twelve males and twelve females, ages 35–69) blood samples were collected and detected; please check supplementary table S1–2 for more information. The individuals provided informed permission for blood sample collection, and their privacy rights were protected.

The experiment was conducted with groups of female BALB/c mice and SD rats, which were randomly divided at the start of the experiment. Anhui Normal University reviewed and approved the study protocols (AHNU-ET2022015).

CRediT authorship contribution statement

Juncheng Wang: Writing – original draft, Visualization, Methodology, Formal analysis, Data curation, Conceptualization. **Meng Liu:** Validation, Methodology, Data curation. **Rukhshan Zahid:** Validation, Methodology, Formal analysis, Data curation, Conceptualization. **Wenjie Zhang:** Methodology, Data curation. **Jiasheng Hao:** Validation, Resources, Project administration. **Yuekang Xu:** Writing – review & editing, Supervision, Resources, Project administration, Funding acquisition, Conceptualization.

Declaration of competing interest

The authors declare that they have no known competing financial interests or personal relationships that could have appeared to influence the work reported in this paper.

Acknowledgment

This study was supported by the National Natural Science Foundation of China Major Research Plan Project (91742101); Anhui International Science and Technology Collaborative Project, China (1604b0602017); Natural Science Foundation of Anhui Province, China (1608085MH160); Scientific research projects of colleges and universities of Anhui Province, China, grant number 2024AH051938.

Appendix A. Supplementary data

Supplementary data to this article can be found online at https://doi.org/10.1016/j.microc.2025.115124.

Data availability

Data will be made available on request.

References

[1] Z. Raisi-Estabragh, L. Szabo, A. Schuermans, A.M. Salih, C.W.L. Chin, H. Vago, A. Altmann, F.S. Ng, P. Garg, S. Pavanello, T.H. Marwick, S.E. Petersen, Noninvasive techniques for tracking biological aging of the cardiovascular system: JACC family series, JACC Cardiovasc. Imaging 17 (2024) 533–551.
[2] J. Fan, T. Watanabe, Atherosclerosis: known and unknown, Pathol. Int. 72 (2022) 151–160.
[3] E. Ji, S. Lee, Antibody-based therapeutics for atherosclerosis and cardiovascular diseases, Int. J. Mol. Sci. 22 (2021).
[4] Z. Li, Y. Zhou, M. Lai, J. Luo, F. Yan, Acoustic delivery of plasma low-density lipoprotein into liver via ApoB100-targeted microbubbles inhibits atherosclerotic plaque growth, ACS Appl. Mater. Interfaces 16 (2024) 24206–24220.
[5] K.A. Sveen, K. Bech Holte, M. Svanteson, K.F. Hanssen, J. Nilsson, E. Bengtsson, T. Julsrud Berg, Autoantibodies against methylglyoxal-modified apolipoprotein B100 and ApoB100 peptide are associated with less coronary artery atherosclerosis and retinopathy in long-term type 1 diabetes, Diabetes Care 44 (2021) 1402–1409.
[6] E. Svenungsson, D. Engelbertsen, M. Wigren, J.T. Gustafsson, I. Gunnarsson, K. Elvin, K. Jensen-Urstad, G.N. Fredrikson, J. Nilsson, Decreased levels of autoantibodies against apolipoprotein B-100 antigens are associated with cardiovascular disease in systemic lupus erythematosus, Clin. Exp. Immunol. 181 (2015) 417–426.
[7] M.K. Choe, H.J. Kim, N.H. Kim, B. Binas, H.J. Kim, Biphasic production of anti-ApoB100 autoantibodies in obese humans and mice, Pharmaceuticals (Basel) 14 (2021).
[8] D. Kounatidis, N.G. Vallianou, A. Poulaki, A. Evangelopoulos, F. Panagopoulos, T. Stratigou, E. Geladari, I. Karampela, M. Dalamaga, ApoB100 and atherosclerosis: what's new in the 21st century? Metabolites 14 (2024).
[9] X. Yi, Y. Wang, Z. Jia, S. Hiller, J. Nakamura, J.C. Luft, S. Tian, J.M. DeSimone, Retinoic acid-loaded poly(lactic-co-glycolic acid) nanoparticle formulation of ApoB-100-derived peptide 210 attenuates atherosclerosis, J. Biomed. Nanotechnol. 16 (2020) 467–480.
[10] Z.T. Berndsen, C.K. Cassidy, The structure of apolipoprotein B100 from human low-density lipoprotein, Nature 638 (2025) 836–843.
[11] Y. Guan, X. Hou, P. Tian, L. Ren, Y. Tang, A. Song, J. Zhao, L. Gao, G. Song, Elevated levels of apolipoprotein CIII increase the risk of postprandial hypertriglyceridemia, Front Endocrinol (Lausanne) 12 (2021) 646185.
[12] J. Behbodikhah, S. Ahmed, A. Elyasi, L.J. Kasselman, J. De Leon, A.D. Glass, A. B. Reiss, Apolipoprotein B and cardiovascular disease: biomarker and potential therapeutic target, Metabolites 11 (2021).
[13] K.H. Burks, N.O. Stitziel, N.O. Davidson, Molecular regulation and therapeutic targeting of VLDL production in Cardiometabolic disease, Cell. Mol. Gastroenterol. Hepatol. 19 (2025) 101409.
[14] K.Y. Chyu, X. Zhao, J. Zhou, P.C. Dimayuga, N.W. Lio, B. Cercek, N.T. Trac, E. J. Chung, P.K. Shah, Immunization using ApoB-100 peptide-linked nanoparticles reduces atherosclerosis, JCI Insight 7 (2022).
[15] P. Duner, I.Y. Mattisson, P. Fogelstrand, L. Glise, S. Ruiz, C. Farina, J. Boren, J. Nilsson, E. Bengtsson, Antibodies against apoB100 peptide 210 inhibit atherosclerosis in apoE(−/−) mice, Sci. Rep. 11 (2021) 9022.
[16] O. McLeod, A. Silveira, G.N. Fredrikson, K. Gertow, D. Baldassarre, F. Veglia, B. Sennblad, R.J. Strawbridge, M. Larsson, K. Leander, B. Gigante, J. Kauhanen, R. Rauramaa, A.J. Smit, E. Mannarino, P. Giral, S.E. Humphries, E. Tremoli, U. de Faire, J. Ohrvik, J. Nilsson, A. Hamsten, Plasma autoantibodies against apolipoprotein B-100 peptide 210 in subclinical atherosclerosis, Atherosclerosis 232 (2014) 242–248.
[17] R.A. Takx, S. Partovi, B.B. Ghoshhajra, Imaging of atherosclerosis, Int. J. Card. Imaging 32 (2016) 5–12.
[18] J. Wang, M. Liu, Z. Cai, R. Zahid, W. Zhang, D. Ma, D. Li, Y. Liang, L. Zha, Y. Zhou, L. Wang, G. Yang, S. Zheng, Y. Xu, Pathogenic epitope-specific monoclonal antibody-based immunoassay for accurate diagnosis and monitoring of tetranectin in sepsis, Int. Immunopharmacol. 143 (2024) 113473.
[19] W. Deng, D. Wang, P. Dai, Y. Hong, J. Xiong, L. Duan, R. Lu, J. Wan, H. Du, B. D. Hammock, W. Yang, Development of a sensitive direct competitive chemiluminescent enzyme immunoassay for gentamicin based on the construction of a specific single-chain variable fragment-alkaline phosphatase fusion protein, Microchem. J. 197 (2024).
[20] R. Wang, S. Fang, D. Wu, J. Lian, J. Fan, Y. Zhang, S. Wang, W. Lin, Screening for a single-chain variable-fragment antibody that can effectively neutralize the cytotoxicity of the *Vibrio parahaemolyticus* thermolabile hemolysin, Appl. Environ. Microbiol. 78 (2012) 4967–4975.
[21] R. Wang, A. Huang, L. Liu, S. Xiang, X. Li, S. Ling, L. Wang, T. Lu, S. Wang, Construction of a single chain variable fragment antibody (scFv) against tetrodotoxin (TTX) and its interaction with TTX, Toxicon 83 (2014) 22–34.
[22] H. Tang, H. Liu, Y. Gao, R. Chen, M. Dong, S. Ling, R. Wang, S. Wang, Detection of alphaB-Conotoxin VxXXIVA (alphaB-CTX) by ic-ELISA based on an epitope-specific monoclonal antibody, Toxins (Basel) 14 (2022).
[23] R. Wang, X. Gu, Z. Zhuang, Y. Zhong, H. Yang, S. Wang, Screening and molecular evolution of a single chain variable fragment antibody (scFv) against Citreoviridin toxin, J. Agric. Food Chem. 64 (2016) 7640–7648.
[24] P. Martviset, J. Thanongsaksrikul, A. Geadkaew-Krenc, S. Chaimon, K. Glab-Ampai, W. Chaibangyang, P. Sornchuer, P. Srimanote, J. Ruangtong, P. Prathaphan, T. Taechadamrongtham, N. Torungkitmangmi, B. Sanannam, C. N. Gordon, N. Thongsepee, V. Pankao, P. Chantree, Production and immunological characterization of the novel single-chain variable fragment (scFv) antibodies against the epitopes on *Opisthorchis viverrini* cathepsin F (OvCatF), Acta Trop. 254 (2024) 107199.
[25] S. Jalilzadeh-Razin, M. Mantegi, M.R. Tohidkia, Y. Pazhang, M.M. Pourseif, J. Barar, Y. Omidi, Phage antibody library screening for the selection of novel high-affinity human single-chain variable fragment against gastrin receptor: an in silico and in vitro study, Daru 27 (2019) 21–34.
[26] J.D. Beatty, B.G. Beatty, W.G. Vlahos, Measurement of monoclonal antibody affinity by non-competitive enzyme immunoassay, J. Immunol. Methods 100 (1987) 173–179.
[27] R. Wang, L. Zeng, H. Yang, Y. Zhong, J. Wang, S. Ling, A.F. Saeed, J. Yuan, S. Wang, Detection of okadaic acid (OA) using ELISA and colloidal gold immunoassay based on monoclonal antibody, J. Hazard. Mater. 339 (2017) 154–160.
[28] H. Tang, Q. Wang, M. Yang, R. Jia, J. Yuan, R. Wang, Development of sensitive immunoassay for identification and detection of mu-KIIIA-CTX: insights into antibody discovery, molecular recognition, and immunoassay, Int. J. Biol. Macromol. 310 (2025) 143346.
[29] H. Tang, H. Liu, R. Chen, Y. Gao, M. Dong, S. Ling, R. Wang, S. Wang, Development of Immunochromatographic strip for detection of alphaB-VxXXIVA-Conotoxin based on 5E4 monoclonal antibody, Toxins (Basel) 14 (2022).
[30] R. Wang, J. Wang, H. Liu, Y. Gao, Q. Zhao, S. Ling, S. Wang, Sensitive immunoassays based on specific monoclonal IgG for determination of bovine lactoferrin in cow milk samples, Food Chem. 338 (2021) 127820.

[31] P. Cai, R. Wang, S. Ling, S. Wang, A high sensitive platinum-modified colloidal gold immunoassay for tenuazonic acid detection based on monoclonal IgG, Food Chem. 360 (2021) 130021.
[32] J. Wang, M. Liu, R. Zahid, W. Zhang, Z. Cai, Y. Liang, D. Li, J. Hao, Y. Xu, Identification of two critical contact residues in a pathogenic epitope from Tetranectin for monoclonal antibody binding and preparation of single-chain variable fragments, Biomolecules 15 (2025).
[33] C. Xie, R. Wang, A. Saeed, Q. Yang, H. Chen, S. Ling, S. Xiao, L. Zeng, S. Wang, Preparation of anti-human Podoplanin monoclonal antibody and its application in Immunohistochemical diagnosis, Sci. Rep. 8 (2018) 10162.
[34] H. Yang, Y. Zhong, J. Wang, Q. Zhang, X. Li, S. Ling, S. Wang, R. Wang, Screening of a ScFv antibody with high affinity for application in human IFN-gamma immunoassay, Front. Microbiol. 9 (2018) 261.
[35] S. Dixit, J. Parashar, R.K. Dhaked, A. Kumar, N. Saxena, Development and validation of streptavidin-biotin-based double antibody sandwich ELISA for ricin diagnosis, Int. Immunopharmacol. 132 (2024) 111986.
[36] A.C. Olivieri, Practical guidelines for reporting results in single- and multi-component analytical calibration: a tutorial, Anal. Chim. Acta 868 (2015) 10–22.
[37] F. Wang, M. Liu, D. Ma, Z. Cai, L. Liu, J. Wang, W. Zhang, L. Zhao, C. Zhai, Y. Xu, Dendritic cell-expressed IDO alleviates atherosclerosis by expanding CD4(+)CD25(+)Foxp3(+)Tregs through IDO-Kyn-AHR axis, Int. Immunopharmacol. 116 (2023) 109758.
[38] F. Wang, L. Liu, J. Wang, M. Liu, W. Zhang, L. Zhao, C. Zhai, Y. Xu, Gain-of-function of IDO in DCs inhibits T cell immunity by metabolically regulating surface molecules and cytokines, Exp. Ther. Med. 25 (2023) 234.
[39] S. Ling, Q. Zhao, M.N. Iqbal, M. Dong, X. Li, M. Lin, R. Wang, F. Lei, C. He, S. Wang, Development of immunoassay methods based on monoclonal antibody and its application in the determination of cadmium ion, J. Hazard. Mater. 411 (2021) 124992.
[40] K. Jia, M. Lin, Q. Zhao, M. Dong, S. Ling, S. Wang, A sensitive and rapid method of lead detection using nanoparticle technology based on monoclonal antibody, Front. Bioeng. Biotechnol. 10 (2022) 962230.
[41] S. Ling, S. Xiao, C. Xie, R. Wang, L. Zeng, K. Wang, D. Zhang, X. Li, S. Wang, Preparation of monoclonal antibody for Brevetoxin 1 and development of Ic-ELISA and Colloidal gold strip to detect Brevetoxin 1, Toxins (Basel) 10 (2018).
[42] N. Jin, S. Ling, C. Yang, S. Wang, Preparation and identification of monoclonal antibody against Citreoviridin and development of detection by Ic-ELISA, Toxicon 90 (2014) 226–236.
[43] L.N. Wei, L. Luo, B. Li, Q.C. Yin, H. Lei, B.Z. Wang, T. Guan, Z.L. Xu, Ultrasensitive "hunter of target": rabbit monoclonal antibody-based competitive lateral flow immunoassay for Saxitoxin, Anal. Chem. 97 (2025) 1410–1418.
[44] Z. Ren, H. Zhang, L. Yang, Z. Wang, J. Xiong, P. Zheng, J. Wang, H. Jiang, Targeted preparation and recognition mechanism of broad-spectrum antibody specific to Aconitum alkaloids based on molecular modeling and its application in immunoassay, Anal. Chim. Acta 1222 (2022) 340011.
[45] Q. Liu, X. Niu, L. Jiang, G. Zhang, P. Wang, S. Zhang, W. Gao, H. Guo, Y. Wang, Y. Li, Double antibody sandwich ELISA based on rabbit monoclonal antibody targeting gD protein for the detection of bovine herpesvirus 1, Int. J. Biol. Macromol. 303 (2025) 140671.
[46] A. Alibakhshi, F. Abarghooi Kahaki, S. Ahangarzadeh, H. Yaghoobi, F. Yarian, R. Arezumand, J. Ranjbari, A. Mokhtarzadeh, M. de la Guardia, Targeted cancer therapy through antibody fragments-decorated nanomedicines, J. Control. Release 268 (2017) 323–334.
[47] H. Lou, X. Cao, Antibody variable region engineering for improving cancer immunotherapy, Cancer Commun (Lond) 42 (2022) 804–827.
[48] N.A. Marston, R.P. Giugliano, G.E.M. Melloni, J.G. Park, V. Morrill, M.A. Blazing, B. Ference, E. Stein, E.S. Stroes, E. Braunwald, P.T. Ellinor, S.A. Lubitz, C.T. Ruff, M.S. Sabatine, Association of Apolipoprotein B-containing lipoproteins and risk of myocardial infarction in individuals with and without atherosclerosis: distinguishing between particle concentration, type, and content, JAMA Cardiol. 7 (2022) 250–256.